LOW-TEMPERATURE ANALOGUE BURNER FACE PLATE TIME RESPONSE

A.R Abu Talib[1], P.T Ireland[2], A.J. Neely[3], A.J Mullender[4] and A.S Mokhtar[1]
[1] Department of Aerospace Engineering, Universiti Putra Malaysia, 43400, Serdang, Selangor, Malaysia
[2] Department of Engineering Science, University of Oxford, OX1 3PJ Oxford, United Kingdom
[3] School of Aerospace, Civil & Mechanical Eng., University of New South Wales, ADFA, ACT 2600, Australia
[4] Rolls-Royce plc., Fire Precautions Group, P.O Box 31, Derby DE24 8BJ, United Kingdom.
Email: abrahim@eng.upm.edu.my

ABSTRACT

This paper presents the measurement of time response of the face plate from a low-temperature analogue burner. To avoid the need for a shutter system as used previously in the pilot low-temperature analogue burner, the burner faceplate has been designed to have a low thermal mass with a time response of less than one second. A thin film mylar face plate was used to replace the thick polycarbonate plate in the design of the compact low-temperature analogue burner. This is to allow a step change of gas temperature of less than one second in the transient heat transfer testing. Calculation of the time response of different thickness of mylar, polycarbonate and PVC face plate materials were presented.

Keywords: *low-temperature analogue burner, face plate, time response.*

INTRODUCTION

In order to represent the ISO2685 [1] burner, it is important to achieve a uniform temperature distribution across the plume at the test plane to match the temperature distribution of the hot flame. The need to minimise the heat losses in the low-temperature analogue burner and to obtain a more uniform temperature profile at the faceplate led the author to design a new compact low-temperature analogue burner [2]. The latter low-temperature analogue burner was designed to improve the low-temperature analogue burner reported in Neely et al. [3] in order to make the test procedure easier, faster and more accurate. The use of a thermally thin faceplate at the burner nozzle eliminated the requirement for a warm up phase and thus avoided the need for a mechanical shutter.

Temperature sensitive liquid crystal has been used extensively in a wide variety of applications [4]. Transient experiments using liquid crystal have been used to measure heat transfer since the 1980's and the technique is now well established. Jones et al. [5] describes the use of liquid crystals in aerodynamic and heat transfer experiments. A recent review of liquid crystal measurements of heat transfer and surface shear stress is given in Ireland and Jones [6]. The transient liquid crystal technique benefits from a sudden change in gas temperature to induce heat transfer. A stainless steel mesh heater [7] used to heat the flow induces a step change to 80°C but this flow must then pass through the analogue burner faceplate. The transient liquid crystal technique using the mesh heater technique also has been successfully used as reported in Abu Talib et al. [8] and Chambers et al. [9].

To avoid the need for a shutter system as used previously in the pilot low-temperature analogue burner [10], the burner faceplate has been designed to have a low thermal mass with a time response of less than one second. The compact design of the analogue burner and the mesh heater improves accessibility for camera views and increases the efficiency of the mesh heater [2]. This new compact design streamlines the test procedure and the robustness of the technique. The compact analogue burner consists of a square cross-section (86 mm x 86 mm internal dimensions) transparent perspex plenum chamber that is 260 mm long, a fast response stainless steel mesh heater, a Rohacell[1] lined square to circular contraction section and a perspex burner nozzle with a 0.13 mm thick mylar[2] burner face. The objective of this paper is to present the detail measurements taken to calculate the face plate time response.

[1] Rohacell® - Polymethacrylimide rigid composite foam.
[2] Mylar: DuPont Films, Mylar® Customer Service, Barley Mill Plaza, P.O. Box 80013, Wilmington, DE 19880-0013.

ISSN 1823-1039 ©2005 FEIIC

MATERIALS AND METHODS

The analogue burner faceplate has been designed to have a small time response and to reproduce the plume shape. The observed temperature rise of the mylar faceplate is actually a function of two time constants, the first due to the heating of the mylar faceplate itself (τ_{mylar}), and the second due to the response of the heater mesh upstream of the faceplate (τ_{mesh}). The analysis of the temperature rise is set out below.

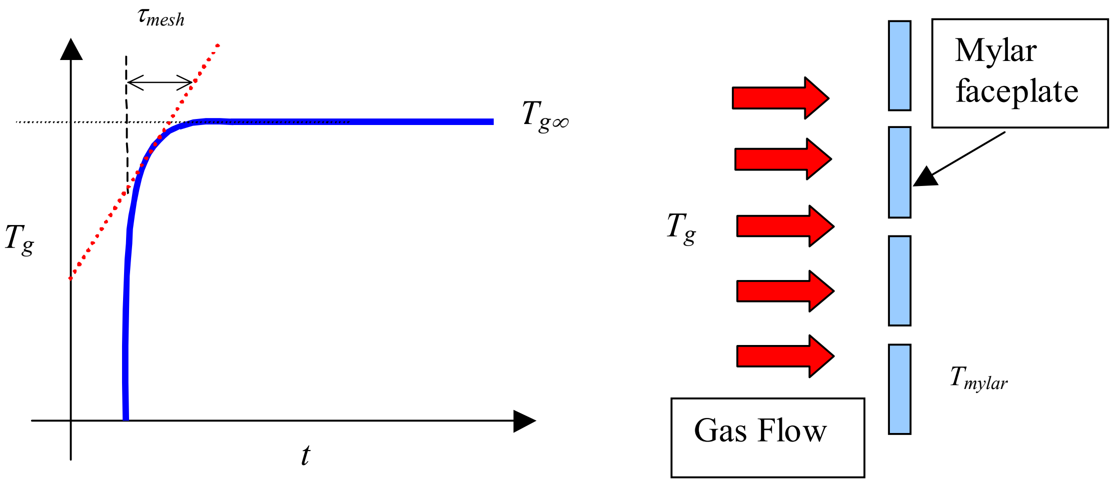

Figure 1: Faceplate time response

The assumptions made in the analysis are as follows:

- The faceplate temperature is time varying but uniform
- The heat transfer between the fluid and the faceplate is determined by a heat transfer coefficient, h.

The rate of increase of mylar temperature with time is related to the heat transferred from the plume by eq. (1). The rate of heat transfer is related to the average heat transfer coefficient by eq. (2).

$$Q = mc\frac{\partial T_{mylar}}{\partial t} \quad (1)$$

$$Q = hA(T_g - T_{mylar}) \quad (2)$$

Where Q is the heat transfer, m is the mylar mass, c is the specific heat capacity, T_{mylar} is the change in surface temperature of the mylar faceplate, T_g is the gas temperature, t is time and A is the area. We can rewrite eq. (1) and eq. (2) as;

$$mc\frac{\partial T_{mylar}}{\partial t} = hA(T_g - T_{mylar}) \quad (3)$$

$$\frac{\partial T_{mylar}}{\partial t} = \frac{hAT_g}{mc} - \frac{hAT_{mylar}}{mc} \quad (4)$$

We define the time constant of the faceplate as $\tau_{mylar} = \dfrac{mc}{hA}$. Eq. (4) becomes;

$$\frac{\partial T_{mylar}}{\partial t} + \frac{T_{mylar}}{\tau_{mylar}} = \frac{T_g}{\tau_{mylar}} \quad (5)$$

However the boundary condition $T_g(t) = T_g\left(1 - e^{-t/\tau_{mesh}}\right)$ has to be applied to account for an exponential increase in the gas temperature [11]. $T_g(t)$ is the change in gas temperature.

Therefore eq. (5) becomes;

$$\frac{\partial T_{mylar}}{\partial t} + \frac{T_{mylar}}{\tau_{mylar}} = \frac{T_g}{\tau_{mylar}} - \frac{T_g e^{-t/\tau_{mesh}}}{\tau_{mylar}} \tag{6}$$

To find the complementary function (C.F) of the differential equation, we must set the right-hand-side (RHS) of eq. (6) to zero.

$$\frac{\partial T_{mylar}}{\partial t} + \frac{T_{mylar}}{\tau_{mylar}} = 0$$

This has a solution $T_{mylar} = Ae^{-t/\tau_{mylar}}$. The particular integral (P.I) is $T_m = C + Be^{-t/\tau_{mesh}}$ where B and C are determined by substitution into eq. (6);

$$-\frac{Be^{-t/\tau_{mesh}}}{\tau_{mesh}} + \frac{C}{\tau_{mylar}} + \frac{Be^{-t/\tau_{mesh}}}{\tau_{mylar}} = \frac{T_g}{\tau_{mylar}} - \frac{T_g e^{-t/\tau_{mesh}}}{\tau_{mylar}}$$

$$Be^{-t/\tau_{mesh}}\left(\frac{1}{\tau_{mylar}} - \frac{1}{\tau_{mesh}}\right) + \frac{C}{\tau_{mylar}} = \frac{T_g}{\tau_{mylar}} - \frac{T_g e^{-t/\tau_{mesh}}}{\tau_{mylar}} \tag{7}$$

Comparing the RHS and LHS in eq. (7):

$$C = T_g \text{ and } B\left(\frac{1}{\tau_{mylar}} - \frac{1}{\tau_{mesh}}\right) = \frac{-T_g}{\tau_{mylar}}.$$

Hence, $$B = T_g\left(\frac{\tau_{mesh}}{\tau_{mylar} - \tau_{mesh}}\right)$$

The general solution becomes;

$$T_{mylar} = Ae^{-t/\tau_{mylar}} + T_g + T_g e^{-t/\tau_{mesh}}\left(\frac{\tau_{mesh}}{\tau_{mylar} - \tau_{mesh}}\right) \tag{8}$$

Initial condition, where $t = 0$: $T_{mylar}(0) = 0$

$$0 = A + T_g + T_g\left(\frac{\tau_{mesh}}{\tau_{mylar} - \tau_{mesh}}\right)$$

$$\Rightarrow A = T_g\left(\frac{\tau_{mylar}}{\tau_{mesh} - \tau_{mylar}}\right)$$

Finally the change in temperature of the mylar faceplate, T_{mylar} can be expressed as

$$T_{mylar} = T_g\left[1 + \left(\frac{\tau_{mylar} e^{-t/\tau_{mylar}} - \tau_{mesh} e^{-t/\tau_{mesh}}}{\tau_{mesh} - \tau_{mylar}}\right)\right] \tag{9}$$

From Gillespie [11], the time response of the mesh heater, τ_{mesh} is correlated as a function of the flow velocity and is expressed as;

$$\tau_{mesh} = \frac{0.111}{u_{mesh}^{0.914}} \tag{10}$$

In this correlation, the flow stream was air. Therefore to use the correlation for the low-temperature analogue burner case, (in which a mixture of helium and air flows through the mesh heater), this equation must be corrected to account for the different density (ρ), viscosity (μ) and gas conductivity (k). The equation governing the thermal response of the mesh heater can be written as;

$$\tau = \frac{mc}{hA} \tag{11}$$

Where m is the wire mass, c is the specific heat, h is the heat transfer coefficient and A is the projected wetted area. τ_1 = air only and τ_2 = helium + air mixture. Dividing τ_2 and τ_1 will result in;

$$\frac{\tau_2}{\tau_1} = \frac{h_1}{h_2} \tag{12}$$

The Nusselt number can be approximated as $Nu = a\,\mathrm{Re}^b\,\mathrm{Pr}^c$ where a, b and c are constants. Nusselt number, $Nu = \frac{hd}{k}$. For Nu_1 / Nu_2 ;

$$\frac{Nu_1}{Nu_2} = \left(\frac{\mathrm{Re}_1}{\mathrm{Re}_2}\right)^b \left(\frac{\mathrm{Pr}_1}{\mathrm{Pr}_2}\right)^c$$

$$\left(\frac{h_1}{h_2}\right) = \left(\frac{\mathrm{Re}_1}{\mathrm{Re}_2}\right)^b \left(\frac{\mathrm{Pr}_1}{\mathrm{Pr}_2}\right)^c \left(\frac{k_1}{k_2}\right)$$

$$\left(\frac{h_1}{h_2}\right) = \left(\frac{\rho_1}{\rho_2}\right)^b \left(\frac{u_1}{u_2}\right)^b \left(\frac{\mu_2}{\mu_1}\right)^b \left(\frac{\mathrm{Pr}_1}{\mathrm{Pr}_2}\right)^c \left(\frac{k_1}{k_2}\right) \tag{13}$$

The values for the b and c are taken from Gillespie (1996), where b = 0.914 and c = 0.333. Eq. (12) becomes;

$$\tau_2 = \tau_1 \left(\frac{\rho_1}{\rho_2}\right)^{0.914} \left(\frac{u_1}{u_2}\right)^{0.914} \left(\frac{\mu_2}{\mu_1}\right)^{0.914} \left(\frac{\mathrm{Pr}_1}{\mathrm{Pr}_2}\right)^{0.333} \left(\frac{k_1}{k_2}\right) \tag{14}$$

RESULTS AND DISCUSSION

The value of τ_1 is found to be 0.306 seconds using eq. (10), which is substituted into eq. (14). Finally we obtained the corrected mesh time response for the low-temperature analogue burner as τ_2 to be 0.118 seconds. The summary of the parameters used in the analysis is shown in Table 1.

Table 1: Properties for air and helium-air mixture at 80°C and 1 atm (101000 Pa)

Analysis Parameters	Air	Helium and air mixture
Density, ρ (kg.m^{-3})	0.997	0.172
Viscosity, μ (kg.m^{-2}.s^{-1})	2.09x10^{-5}	2.23x10^{-5}
Thermal conductivity, k (W.m^{-1}.K^{-1})	0.030	0.160
Specific heat capacity, c (J.kg^{-1}.K^{-1})	1392	5041
Prandtl number, Pr $\left(\frac{\mu c}{k}\right)$	0.961	0.706
Mass flow rate, $\dot{m}$ (kg.s^{-1})	0.0026	0.0014
Velocity through the mesh, u (m.s^{-1})	0.33	1.05

Faceplates made from different types of materials and different thicknesses were fitted to the analogue burner nozzle to measure their time response. The overall time response of the faceplate and mesh combination was measured by capturing infrared images of the faceplate from the start of the transient test. The temperature history of the faceplate can be deduced from the infrared image sequence. An emissivity value of $\varepsilon = 0.9$ was used for all faceplate materials. The transport delay between the mesh and the faceplate is found to be 0.11 seconds as shown in Table 2. This transport delay has to be added to the measured time history of the faceplate obtained from the infrared camera.

Table 2: Transport delay from the mesh to the faceplate

Distance between the mesh and the faceplate, s (m)	0.117
Flow velocity through the mesh, u (m.s^{-1})	1.05
Transport delay, $t_d = s / u$ (s)	0.11

The measured surface temperature histories from each faceplate material obtained from the infrared camera were matched to eq. (15) by selecting the mylar time constant τ_m.

$$T_{bestfit} = T_0 + \left(T_{g\infty} - T_0\right)\left(1 + \left(\frac{\tau_m}{\tau_{mesh} - \tau_m}\right)e^{-t/\tau_r} - \left(\frac{\tau_{mesh}}{\tau_{mesh} - \tau_m}\right)e^{-t/\tau_{mesh}}\right) \tag{15}$$

Here T_o is the initial starting temperature, $T_{g\infty}$ is the asymptotic gas temperature and τ_{mesh} is 0.118 seconds. Figure 2 shows the measured temperature history for different type of faceplate materials and thickness obtained from infrared (IR) camera.

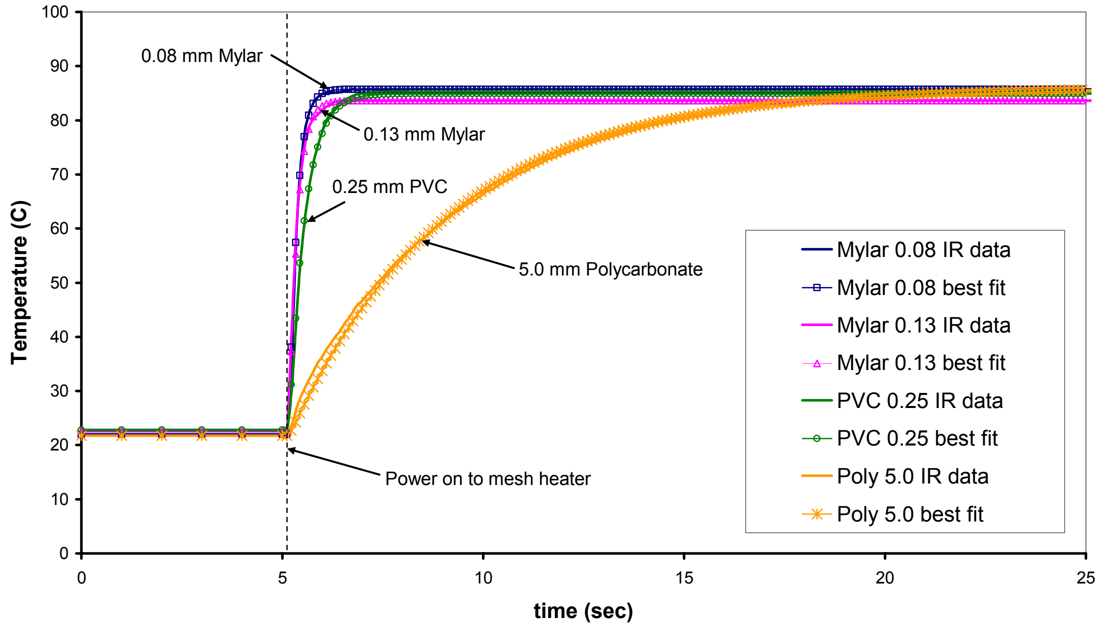

Figure 2: Measured temperature history for different type of faceplate materials and thickness obtained from infrared camera

The original pilot low-temperature analogue burner used 5 mm thick polycarbonate. The time response for the polycarbonate faceplate was found to be over 7 seconds determined from eq. (15). The thickness of the faceplate governs the thermal mass of the material and, not surprisingly, it was found that the thin mylar faceplates had shorter time constants than the original thick polycarbonate. Figure 3 shows a plot of faceplate thickness against time response for different faceplate materials. This is sensible if it is assumed that there are only small changes in the faceplate density (ρ), specific heat capacity (c) and heat transfer coefficient (h) for the different type of materials.

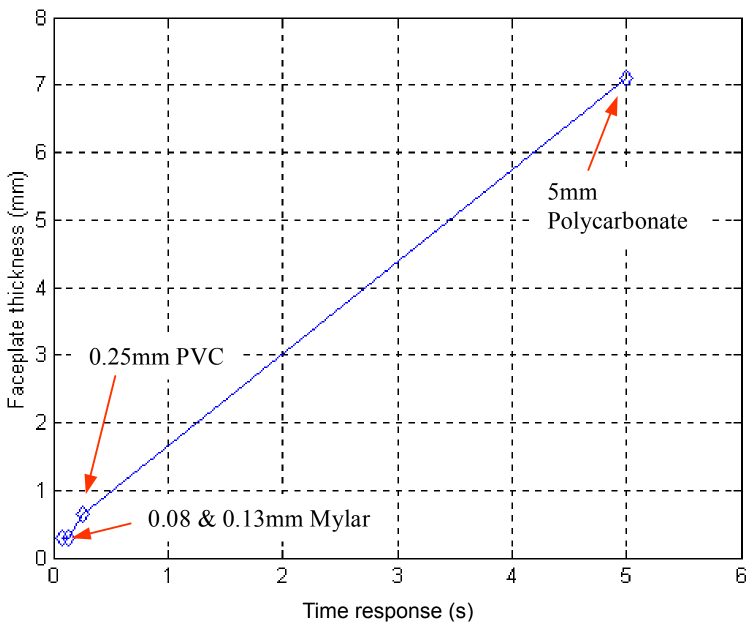

Figure 3: Thickness versus time response

The time response for the 0.08 mm and 0.13 mm thick mylar are both observed to be 0.33 and 0.35 seconds respectively. These are sufficiently small to enable the use of the step change assumptions in the transient thermal analysis. The summary of the time response of the different type of faceplate materials are shown in Table 3. Abu Talib reported that the thin mylar sheets were not deflected during the operation of the low-temperature burner and the effect of deflection can be neglected.

Table 3: Time response for different faceplate materials

Material	Thickness (mm)	Time response (s)
Mesh heater	-	0.12
Mylar faceplate	0.08	0.33
Mylar faceplate	0.13	0.35
PVC faceplate	0.25	0.69
Polycarbonate faceplate	5.00	7.20

CONCLUSION

This paper has described the application of a thermally thin mylar faceplate to the compact low-temperature analogue burner design. The time response of the mylar face plate of 0.13 mm thickness was found to be 0.35 second. With its short time response, it is sufficient to allow a step change in temperature for the transient heat transfer experiment.

ACKNOWLEDGEMENT

The authors wish to thank the UK Ministry of Defence (MoD) and the UK Departmental of Trade and Industry (DTI) for their financial support for this work through the Defence Evaluation and Research Agency (DERA), Pyestock. The first author thanks the Malaysian Government and the University Putra Malaysia for their financial support.

REFERENCES

[1] The International Organisation for Standardisation (1992) Aircraft - Environmental Conditions and Test Procedures for Airborne Equipment - Resistance to Fire in Designated Fire Zones, ISO2685:1992(E).

[2] Abu Talib, A.R., Neely, A.J., Ireland, P.T. and Mullender, A.J. (2001) Compact Low-Temperature Analogue of Aero Engine Fire-Certification Burner, Proceedings, ASME/IGTi Turbo Expo, New Orleans, Louisiana, USA, 2001-GT-0364.

[3] Neely, A.J., Ireland, P.T. and Mullender, A.J. (1998), Validation of Novel Low-Temperature Fire Event Modelling Technique, Proceedings, Royal Aeronautical Society Conference - Verification of Design Methods by Test and Analysis, London, UK.

[4] Ireland, P.T. and Jones, T.V. (1986) Detailed Measurements of Heat Transfer on and Around a Pedestal in Fully-Developed Channel Flow, Proceedings, 8th International Heat Transfer Conference, San Francisco, USA, 975-986.

[5] Jones, T.V., Wang, Z. and Ireland, P.T. (1992) Liquid Crystals in Aerodynamic and Heat Transfer Testing, Proceedings, IMechE Conference - Optical Methods and Data Processing in Heat and Fluid Flow, City University, London, UK.

[6] Ireland, P.T. and Jones, T.V. (2000) Liquid Crystal Measurements of Heat Transfer and Surface Shear Stress, Measurement Science Technology, **11**: 969-986.

[7] Gillespie, D.R.H., Wang, Z. and Ireland, P.T. (1995), Heating Element, PCT/GB96/02017, UK.

[8] Abu Talib, A.R., Neely, A.J., Ireland, P.T and Mullender, A.J (2004) A novel liquid crystal image processing technique using multiple gas temperature steps to determine heat transfer coefficient distribution and adiabatic wall temperature. Journal of Turbomachinery, **126**(4): 587-596.

[9] Chambers, A.C., Gillespie, D.R.H., Ireland, P.T. and Dailey, G.M. (2002) A Novel Transient Liquid Crystal Technique to Determine Heat Transfer Coefficient Distributions and Adibatic Wall Temperature in a Three Temperature Problem, Proceedings, ASME/IGTi Turbo Expo, Amsterdam, The Netherlands, GT-2002-30532

[10] Neely, A.J., Ireland, P.T. and Mullender, A.J. (1999), Pilot Study to Investigate Novel Experimental and Theoretical Fire-Event Modelling Techniques, Proceedings, 37th Aerospace Science Meeting, Reno, Nevada, USA, AIAA-99-09-0326.

[11] Gillespie, D.R.H. (1996) Intricate Internal Cooling Systems for Gas Turbine Blading, D.Phil Thesis, Department of Engineering Science University of Oxford, Oxford, UK.

[12] Abu Talib, A.R. (2003) Detailed Investigation of the Low-Temperature Analogy of an Aircraft Engine Standard Fire-Test, D.Phil Thesis, Department of Engineering Science, University of Oxford, U.K.

NOMENCLATURE

A	area	(m^2)
c	specific heat capacity	($J.kg^{-1}K^{-1}$)
d	diameter	(m)
h	heat transfer coefficient	($W.m^{-2}.K^{-1}$)
k_l	pressure drop loss coefficient	
m	mass	(kg)
$\dot{m}$	mass flow rate	($kg.s^{-1}$)
Nu	Nusselt number, $\mathrm{Nu} = \frac{hd}{k}$	
Pr	Prandtl number, $\mathrm{Pr} = \frac{c\mu}{k}$	
Q	total heat transfer	(W)
Re	Reynolds number, $\mathrm{Re} = \frac{\rho u d}{\mu}$	
s	distance between mesh heater and face plate	(m)
t	time	(s)
t_d	transport delay	(s)
T_g	maximum gas temperature	(°C)
$T_{g\infty}$	asymptotic gas temperature	(°C)
T_{mylar}	mylar faceplate surface temperature change	(°C)
u	velocity	($m.s^{-1}$)
u_{mesh}	velocity through the mesh heater	($m.s^{-1}$)

<u>Greek</u>

ρ	density	($kg.m^{-3}$)
μ	dynamic viscosity	($kg.m^{-2}.s^{-1}$)
β	porosity	
ε	emissivity	
τ_1	time constant for air only flow	(s)
τ_2	time constant for mixture of helium and air flow	(s)
τ_{mesh}	mesh heater time constant	(s)
τ_{mylar}	mylar faceplate time constant	(s)